Rapport BIPM-82/2

REPORT ON THE INTERNATIONAL COMPARISON OF ACTIVITY MEASUREMENTS OF A SOLUTION OF ^{55}Fe (February 1979)

by

D. SMITH and M.J. WOODS

National Physical Laboratory
Teddington, Middlesex TW11 0LW, United Kingdom

February 1982

Bureau International des Poids et Mesures
Pavillon de Breteuil, F-92310 SEVRES

CONTENTS

Abstract

The Bureau International des Poids et Mesures organised an international comparison for the measurement of the radioactivity concentration of a ^{55}Fe solution. The National Physical Laboratory was charged with the preparation and distribution of the solution and with the collation of the results. The active material was supplied by the National Accelerator Centre and purity-checked by the Laboratoire de Métrologie des Rayonnements Ionisants and the Physikalisch-Technische Bundesanstalt. The solution was distributed in December 1978.

The numerous methods of measurement for activity and K X-ray-emission rate are described and the results obtained are presented. Details on source preparation, counting equipment, experimental corrections, results and uncertainties are reported in tabular or graphical form. In addition, the product of the K-shell capture probability and the K-shell fluorescence yield ($P_K \omega_K$) has been determined as 0.283 ± 0.002.

1. Introduction

Following a decision taken by Section II (Mesure des radionucléides) of the Comité Consultatif pour les Etalons de Mesure des Rayonnements Ionisants (CCEMRI), the Bureau International des Poids et Mesures (BIPM) organised an international comparison to take place in 1978/79 for the measurement of the activity concentration of a ^{55}Fe solution. As recent international comparisons [1-3] involved γ-ray emitting nuclides and had shown a steady and satisfactory decrease in the spread of the results, it was thought appropriate to attempt an intercomparison of a nuclide which could not be measured in the BIPM ionization-chamber reference system. ^{55}Fe, which decays by pure electron capture [4], represents such a nuclide (see decay scheme, Fig. 1).

Eleven laboratories (listed in Table 1 with their abbreviations) participated, using various methods of measurement, and presented a total of 18 results. The NPL was charged with organising the preparation and distribution of the solution, and with the collation of the results of the measurements.

2. Preparation and distribution of the solution

The primary ^{55}Fe was procured by NAC, who supplied NPL with approximately 1 000 MBq of ^{55}Fe in the form of a carrier-free aqueous solution of HCl (2 mol per dm^3). Two samples of this solution, each comprising about 7.5 MBq, were dispatched to LMRI and PTB for purity checks. The only significant impurity detected by both laboratories was ^{54}Mn and the relative impurity level at the reference date of the intercomparison was quoted as

LMRI: $(0.96 \pm 0.02)\ 10^{-6}$,

PTB : $(1.08 \pm 0.05)\ 10^{-6}$.

The stock solution was diluted at NPL to provide an activity concentration of approximately 4 MBq/g, with a final carrier content of 20 μg per gramme of Fe in an aqueous solution of HNO_3 (0.1 mol per dm^3). Each participant was supplied with two flame-sealed 5 ml glass ampoules, each containing about 3 ml of the diluted solution. The only data supplied to the participants was the recommended half-life value of 2.70 years and the reference date of the intercomparison 1979-02-01, 0 h UT. The measurements were carried out in the first half of 1979.

3. Methods of measurement

Since there was no preferred method of measurement, the participants were free to use whatever technique they desired, and to provide as much information as they felt appropriate for their chosen methods. In collating the results, it became evident that further information regarding some of the methods would be useful, and this was sought and obtained from the participants.

Although many different techniques were employed, the methods can be classified into those which result in an estimate of activity (N_o) and those which result in an estimate of the emission rate of K X-rays (N_{KX}). These quantities are, of course, related by the equation

$$N_o = \frac{N_{KX}}{P_K \omega_K} .$$

The methods of measurement are described below, and details of counting equipment, conditions of measurement and various corrections applied are given in Tables 2 to 5.

Each method of each laboratory is referred to by a number ranging from (1) to (18).

3.1. Measurements of N_o

AECL (1); BCMN (2) and PTB (3) calibrated the X-ray response of a solid-state detector in terms of the known activity of nuclides, such as ^{51}Cr and ^{54}Mn. NPL (4) and NRC (5) used efficiency extrapolation with ^{51}Cr and ^{54}Mn as tracers in $4\pi\beta$(gas-filled proportional counter)-γ counting systems. LMRI (6) used $4\pi\beta$(pressurised proportional counter)-γ counting with ^{54}Mn as a tracer, using covered sources so only K X-rays were detected. LMRI (7) and IBJ (8) used $4\pi\beta$(liquid sinctillation)-γ efficiency extrapolation with ^{54}Mn as a tracer. NAC (9) used $4\pi\beta$(liquid scintillation)-γ with theoretical efficiency functions for ^{55}Fe, ^{54}Mn and ^{51}Cr. BCMN (10) used $4\pi\beta$(liquid scintillation) with two phototubes connected in summation and in coincidence.

Seven of the ten methods for N_o (i.e. all except 4, 5 and 10) involve assuming the value of P_K or ω_K, or assuming that either or both of these parameters vary smoothly with atomic number. It should be noted, however, that in all these cases the final estimate of N_o depends only on the ratio of P_K (or ω_K) for ^{55}Fe to that for the various tracer nuclides used.

The methods are now described in more detail.

3.1.1. AECL (1) used X-ray counting with sources sandwiched between two thin NaI(Tl) detectors calibrated in terms of the ratio (observed K X-rays/known activity) as a function of atomic number for the nuclides ^{51}Cr, ^{54}Mn and ^{57}Co. Each detector output was fed to a single-channel analyser, the window of which was selected to avoid noise and higher-energy γ rays, and then to a scaler. Pulses outside the window were ignored, but should cancel in the calibration. Corrections were made for true coincidence summing [5] (e.g. 33% for ^{57}Co) and background. The reference sources were of similar activity to ^{55}Fe and prepared in a similar manner, so source self-absorption could be incorporated into the efficiency curve, and most other sources of uncertainty should cancel in this relative counting method. A value of X-ray count rate/activity of 0.178 5 ± 0.7% was interpolated from the calibration curve (Fig. 2). Most sources were prepared from a ten-fold dilution of the ^{55}Fe solution. However, the undiluted solution gave a count rate per gramme which was 0.27% lower than the diluted solution, indicating that self absorption is not very different over this range of carrier concentration. The N_o value deduced from the efficiency curve assumes that $P_K\omega_K$ changes smoothly with atomic number, although the actual values were not used.

3.1.2. BCMN (2) calibrated a Si(Li) detector in terms of

$$\varepsilon = \frac{\text{observed K X-ray count rate}}{N_o P_K \omega_K}$$

as a function of atomic number, for ^{51}Cr, ^{54}Mn, ^{57}Co and ^{65}Zn, ensuring that all the sources were prepared in the same way and with similar carrier concentration. The detector efficiency for Mn K X-rays, which includes source self-absorption, was interpolated as ε = 0.030 7, with 0.7% uncertainty (Fig. 2), and so

$$N_o = \frac{\text{observed K X-ray count rate from } ^{55}Fe}{\varepsilon P_K \omega_K} .$$

BCMN also compared ^{55}Fe directly to ^{54}Mn, when

$$N_o(^{55}Fe) = N_o(^{54}Mn) \frac{(\text{count rate } ^{55}Fe)}{(\text{count rate } ^{54}Mn)} \frac{P_K\omega_K\ (^{54}Mn)}{P_K\omega_K\ (^{55}Fe)} \frac{\varepsilon(^{54}Mn)}{\varepsilon(^{55}Fe)} ,$$

where $\frac{\varepsilon(^{54}Mn)}{\varepsilon(^{55}Fe)} = 0.965 \pm 0.002.$

No systematic differences were observed between measurements at four dilutions (with factors 1, 2, 4 and 8). For both methods the N_o value deduced depends on the ratio of assumed $P_K\omega_K$ values.

3.1.3. PTB (3) calibrated an intrinsic Ge detector in terms of

$$\varepsilon = \frac{\text{observed K X-ray count rate}}{N_o P_K}$$

as a function of atomic number for ^{51}Cr, ^{54}Mn and ^{58}Co, measured under similar conditions. From this smooth, almost linear function which incorporated source self-absorption and the quantity ω_K, the value for ^{55}Fe was interpolated as 1.35×10^{-3} with 1.5% uncertainty (Fig. 2). The activity was calculated as

$$N_o = \frac{\text{observed K X-ray count rate for } ^{55}Fe}{\varepsilon P_K} .$$

Two sets of measurements were made, one with 'drop' sources (weighed), the other with electroplated sources. The effective drop masses of the latter were found by comparing the γ-radiation from electrolytic and drop sources. For ^{55}Fe electrolytic sources, a known amount of ^{59}Fe was added to the ^{55}Fe solution for this purpose.

The ^{55}Fe activity deduced depends on the ratio of P_K values used and also assumes that ω_K varies smoothly with atomic number.

3.1.4. NPL (4) used efficiency extrapolation with ^{51}Cr and ^{54}Mn as tracers in a $4\pi\beta$(Ar-CH_4 filled proportional counter)-γ coincidence counting system. The counter operated at atmospheric pressure and the efficiency (maximum 58%) was varied by the addition of absorbing material. Discrimination therefore took place over the low-energy Auger electron-photon spectrum and also over some high-energy K X-rays due to partial K X-ray absorption in the atmospheric-pressure detector. A linear extrapolation was made to 100% counting efficiency, as shown in Fig. 2.

To improve the maximum efficiency, the technique [6] of drying the drop sources in an NH_3 atmosphere was adopted. In this method one drop of Catanac (50 µg per gramme of water) was added to each source, which was then dried, redissolved in water and dried in the vapour from NH_4OH. Small changes in source efficiency were made by sublimating NH_4Cl vapour onto the source, and larger changes by addition of VYNS foils.

The method was checked by measuring the activity of ^{51}Cr by direct methods and by tracing with ^{54}Mn; a difference of only 0.2% was found.

3.1.5. NRC (5) used efficiency extrapolation with ^{51}Cr and ^{54}Mn as tracers in a $4\pi\beta$(Ar-CH_4 filled proportional counter)-γ anticoincidence [7] counting system. The counter was pressurized to 1 000 kPa to ensure essentially total K X-ray absorption, and the efficiency (maximum 70%) was altered by electronic discrimination over the low-energy Auger electron-photon spectrum. A linear extrapolation, as defined by the χ^2 test, was made to 100% counting efficiency. A typical data set is shown in Fig. 2.

The method was checked by measuring the activity of ^{51}Cr by direct methods and by tracing with ^{54}Mn; agreement to within 0.5% was obtained.

3.1.6. LMRI (6) used a $4\pi\beta$(Ar-CH_4 filled proportional counter)-γ coincidence method with ^{54}Mn as a tracer. The proportional counter was pressurised to 700 kPa. The sources were covered with 400 $\mu g/cm^2$ foil so that only K X-rays were detected, hence the total observed count rate of ^{55}Fe plus tracer is

$$N_{XT} = N_o^{55} T_K^{55} \varepsilon_{KX}^{55} + N_o^{54} \{T_K^{54} \varepsilon_{KX}^{54} + (1 - T_K^{54} \varepsilon_{KX}^{54}) \varepsilon_{\beta\gamma}\} ,$$

where
T_K = probability of K X-ray emission and interaction in the counter,
ε_{KX} = probability of counting the K X-rays which have interacted in the counter.

The observed K X-ray-γ coincidence rate gives

$$\frac{N_c}{N_\gamma} = T_K^{54} \varepsilon_{KX}^{54} ,$$

wherefrom

$$N_o^{55} = \frac{\varepsilon_{KX}^{54}}{\varepsilon_{KX}^{55}} \frac{T_K^{54}}{T_K^{55}} \{N_{XT} \frac{N_\gamma}{N_c} - N_o^{54} (\frac{N_\gamma}{N_c} - 1) \varepsilon_{\beta\gamma}\} .$$

If the counter gain is high enough, ε_{KX}^{54} and ε_{KX}^{55} are very close to unity and it can be assumed that $\frac{\varepsilon_{KX}^{54}}{\varepsilon_{KX}^{55}} = 1$. Thus, efficiency variation and extrapolation are not involved in this method, but instead each term in the above equation is simply replaced by its value.

The N_c/N_γ ratios were about 0.235.

The values of $\varepsilon_{\beta\gamma}$ and N_o^{54} are determined from a standardization of ^{54}Mn alone.

The probability can be expressed as

$$T_K = P_K \omega_K t_K f_K ,$$

where
t_K = transmission of X-rays through the film supporting the source,
f_K = probability of X-rays being counted by the detector.

A Monte-Carlo simulation was used to estimate t_K and f_K for both ^{55}Fe and ^{54}Mn and gave

$$t_K^{54}/t_K^{55} = 0.985\ 8 \pm 0.000\ 5, \quad f_K^{54}/f_K^{55} = 1.001\ 5 \pm 0.000\ 5.$$

Using the $P_K\omega_K$ values in Table 3 then gives

$$T_K^{54}/T_K^{55} = 0.912 \pm 0.027.$$

The N_o value depends on the ratio of assumed $P_K\omega_K$ values.

3.1.7. LMRI (7) also used $4\pi\beta$(liquid scintillation)-γ efficiency extrapolation with ^{54}Mn as a tracer. Noting that only K events have sufficient energy to be finally detected, the total count rate for ^{55}Fe plus tracer is

$$N_{KT} = N_o^{55}\ S_K^{55}\ \varepsilon_K^{55} + N_o^{54}\ \{S_K^{54}\ \varepsilon_K^{54} + (1 - S_K^{54}\ \varepsilon_K^{54})\ \varepsilon_{\beta\gamma}\},$$

where
S_K = probability of K emission and interaction in the counter,
ε_K = probability of counting K emissions which have interacted in the counter.

The observed coincidence rate gives

$$\frac{N_c}{N_\gamma} = S_K^{54}\ \varepsilon_K^{54} = \varepsilon_\beta .$$

The method assumes that $\varepsilon_K^{55} \to 1$ as $\varepsilon_K^{54} \to 1$ and that the ratio $\frac{\varepsilon_K^{55}}{\varepsilon_K^{54}}$ can be expressed as a polynomial in the observed efficiency, i.e.

$$y = \frac{S_K^{54}}{S_K^{55}} \{N_{KT} - N_o^{54}\ (1 + \frac{1 - \varepsilon_\beta}{\varepsilon_\beta}\ \varepsilon_{\beta\gamma})\} = N_o^{55}\ \{1 + f(\varepsilon_\beta)\},$$

where $\frac{\varepsilon_K^{55}}{\varepsilon_k^{54}} = 1 + f(\varepsilon_\beta) \to 1$ as $\varepsilon_\beta \to S_K^{54}$.

The function y is therefore extrapolated to $\varepsilon_\beta = S_K^{54}$. The values of $\varepsilon_{\beta\gamma}$ and N_o^{54} are determined from a standardisation of ^{54}Mn alone.

The probability S_K can be expressed as

$$S_K = P_K(1 - \omega_K + p\omega_K),$$

where p = probability of K X-rays interacting in the counter.

The values of $P_K\omega_K$ are assumed (Table 3) and p (≈ 0.9) is calculated by Monte-Carlo simulation, giving $S_K^{54} = 0.871$ and $\frac{S_K^{54}}{S_K^{55}} = 1.024 \pm 1\%$.

The efficiency ε_β varied in 12 steps from 3% to 50%, and a quadratic extrapolation was made to the point $\varepsilon_\beta = 87.1\%$.

The activity deduced depends on the ratio of P_K values assumed, and to a lesser extent on the ratio of ω_K values assumed.

3.1.8. IBJ (8) used a $4\pi\beta$(liquid scintillation)-γ efficiency extrapolation with ^{54}Mn as a tracer. Since the detector will only observe K events, the total count rate for ^{55}Fe plus tracer is

$$N_{KT} = N_o^{55}\,\varepsilon^{55} + N_o^{54}\,\{\varepsilon_\beta + (1 - \varepsilon_\beta)\,\varepsilon_{\beta\gamma}\}\ ,$$

where $\varepsilon_\beta = \frac{N_c}{N_\gamma}$,

N_c = observed coincidence rate,

ε^{55} = probability of K emission and detection of ^{55}Fe.

Thus

$$y = \frac{N_{KT}}{\varepsilon_\beta} - N_o^{54}\,(1 + \frac{1 - \varepsilon_\beta}{\varepsilon_\beta}\,\varepsilon_{\beta\gamma}) = N_o^{55}\,\frac{\varepsilon^{55}}{\varepsilon_\beta}\ .$$

The method assumes that as $\varepsilon_\beta \to 1$, $\varepsilon^{55} \to \frac{P_K^{55}}{P_K^{54}}$, so extrapolation of the function y is made to $\varepsilon_\beta = 1$. The values of N_o^{54} and $\varepsilon_{\beta\gamma}$ are known from a standardisation of ^{54}Mn alone (Fig. 2).

The observed efficiency was varied from 6% to 21.5% by changing the voltage applied to the phototube, and the extrapolation was found to be linear.

3.1.9. NAC (9) applied a $4\pi\beta$(liquid scintillation)-γ coincidence method, using ^{54}Mn and ^{51}Cr to determine the efficiency. It is <u>not</u> an extrapolation method and relies entirely on the theoretical relationship (based on the work of Gibson and Marshall [8]) between the efficiencies for the three radionuclides. For a mixed ^{55}Fe-tracer source, the total scintillator count rate and tracer efficiency N_c/N_γ is measured. The contribution from the tracer is subtracted in the usual manner. The theoretical relation between ε^{55} and the tracer efficiency is calculated. In finding this function, the zero probability is calculated as a function of the figure of merit P, as defined in ref. [8]. The efficiency for ^{55}Fe corresponding to the efficiency of the tracer is found from this function, so that

$$N_o^{55} = \frac{\text{count rate for } ^{55}\text{Fe}}{\text{efficiency deduced for } ^{55}\text{Fe}}\ .$$

A maximum tracer efficiency of 50% for ^{54}Mn and 46% for ^{51}Cr was obtained. The ^{55}Fe activity values deduced from the measurements with the two tracers differed by 0.75%. In addition, they depend on the ratio of P_K values assumed. Further details can be found in a CSIR report [9].

3.1.10. BCMN (10) used a $4\pi\beta$(liquid scintillation) system with two phototubes to observe the scintillations. The method relies on a theoretical relationship between the count rates with the two phototubes in coincidence or in summing mode. A Poisson distribution is assumed for the number of photoelectrons emitted from the cathode. The probability that at least one electron reaches a dynode of either phototube is $1 - e^{-m}$, where m is the mean number of photoelectrons hitting the two first dynodes. For the matched phototubes, the probability of one electron reaching the first dynode of one phototube is $1 - e^{-m/2}$. If the detection efficiency in coincidence and in summing modes is respectively ε_c and ε_s, then

$$\varepsilon_s = 1 - e^{-m}, \quad \varepsilon_c = (1 - e^{-m/2})^2 \quad \text{and} \quad \varepsilon_s/\varepsilon_c = (1 + e^{-m/2})/(1 - e^{-m/2}).$$

A measurement of $\varepsilon_s/\varepsilon_c$ therefore gives the parameter m and hence determines both ε_c and ε_s separately.

The results are based principally on the coincidence count-rate, since in that case the uncertainty in the background correction is negligible. Then

$$N_o = (\text{count rate in coincidence})/\varepsilon_c \ .$$

Measurements obtained with two different scintillators for twelve samples prepared from three different dilutions gave mean values as follows

	ε_c (%)	ε_s (%)	N_o (s^{-1} mg^{-1})
Lumagel	53.1	92.6	3 920 ± 36
Toluene cocktail	38.6	85.7	3 810 ± 40

The 3% difference in N_o is presumably due to inadequacy of the statistical model. It was assumed that the correction for this would be linear with efficiency, so that an extrapolation of the results to $(1 - \varepsilon_c)/\varepsilon_c \to 0$ and separately to $(1 - \varepsilon_s)/\varepsilon_s \to 0$ was made.

The two intercepts differed by only 1%, and the mean value was adopted (Fig. 2).

3.2. Measurement of N_{KX}

Five laboratories (BCMN(11), LMRI(12), NPL(13), IMM(14,16) and AIEA(15)) used a gas-filled pressurised proportional counter and two (LMRI(17) and NBS(18)) used a defined-solid-angle method with a thin-window NaI detector.

3.2.1. Pressurised proportional-counter methods

Four laboratories (BCMN(11), LMRI(12), NPL(13) and IMM(14)) used a 4π counter and two (AIEA(15) and IMM(16)) used a 2π counter. All the counters were filled with Ar-CH_4 and all participants sandwiched the sources with material sufficient to stop all Auger electrons and L X-rays. The 4π counters were operated at a high pressure, sufficient to stop all K X-rays. The corrections applied in this method are for

- X-ray absorption in the foils covering the source. This varied from 2% to 5% and was either calculated from theory $\left[\int_0^{\pi/2} \exp(-\mu t/\cos\theta)\, \sin\theta\, d\theta\right]$ or from a combination of theory with a knowledge of the additional absorption when a further foil was added.

- Source self-absorption of K X-rays. This varied from 0.1% to 2% and was estimated in different ways (see Table 4 - except AIEA with electroplated sources). IMM and NPL used the technique of drying sources in NH_3 [6] to minimise absorption.

- Extrapolation to zero energy from the lower threshold of measurement, amounting typically to about 0.3%.

3.2.2. Further details of the 2π methods

AIEA(15) used a pressure of 130 kPa, which allows some X-ray escape. A correction of (2.04 ± 0.03)%, deduced from measurements up to 300 kPa, was applied to obtain the saturation value. AIEA used electroplated sources to eliminate self absorption, and determined the effective drop masses by using a mixture of ^{55}Fe with a known amount of ^{59}Fe (activity ratio 10 to 1), so that the γ emission from electroplated and from weighed sources could be compared with a NaI detector. The spectrum was counted only up to 12 keV, to keep the contribution from the ^{59}Fe spectrum to a minimum (- 3% correction for ^{59}Fe events below 12 keV, and + 4% for ^{55}Fe events above 12 keV). A lower discrimination level of 1 keV was used, but no correction to zero energy was made.

IMM(16) used the "method of multiple fillings", with pressures up to 90 kPa. In principle four fillings are used, for example 4 kPa CH_4 (count rate M_1); 8 kPa CH_4 (rate M_2); 4 kPa CH_4 + 40 kPa Ar (rate N_1); 8 kPa CH_4 + 80 kPa Ar (rate N_2).

The count rates N_1 and N_2 are corrected for

- background (with no source),

- "film effect", i.e. photoelectrons emitted into the gas following K X-ray absorption in the film, calculated theoretically as about 0.2% of the total K X-rays,

- "wall effect" ($\approx$ 0.1%), i.e. photoelectrons emitted from counter walls following K X-ray absorption by wall material, calculated as W (fraction of X-rays reaching the wall $\approx 1 - \frac{N_i}{N_{KX}}$), where W is deduced

as follows:

M_2 = background + X-rays absorbed in CH_4 + film effect + W
= background + $2(M_2 - M_1)$ + (0.000 2) • (number of K X-rays) + W.

The corrected rates N_i can be expressed [10] in terms of the count rate at infinite pressure N_∞ as

$$N_1 = N_\infty (1 - e^{-\mu d}) \quad \text{and} \quad N_2 = N_\infty (1 - e^{-\mu\, 2d}) ,$$

where d and 2d represent the quantity of absorbing gases, and where spherical symmetry is assumed.

The exponential can be eliminated to give

$$N_\infty = N_1/(2 - N_2/N_1) .$$

3.2.3. The defined solid angle method

LMRI(17) and NBS(18) used a thin NaI(Tl) detector with a Be-Al window, where the solid angle is defined by a collimator.

In the LMRI system, the space between source and detector is filled with helium at ambient pressure. The weighed sources were sandwiched between thick mylar films. The calculated corrections applied totalled to (13.0 ± 1.7)% for the absorption in the mylar, Be, etc. As an empty spectrum was observed below the escape peak, no correction was necessary for counts below the lower energy threshold used. The source self-absorption was estimated to be lower than 0.05%.

NBS used both weighed and electroplated uncovered sources, and applied calculated corrections totalling (8.2 ± 0.5)% for the absorption in the Be, and a (3.9 ± 0.6)% correction for the extrapolation to zero energy. Two methods were used to avoid or estimate self absorption:

- Firstly an electroplated source was counted by the defined-solid-angle detector [11]. The plated source was taken into solution and used to calibrate the efficiency of a liquid-scintillation system, which was then used to measure the K X-ray emission rate per gramme of the BIPM solution. This intercomparison step contributed an uncertainty of about 0.2%.

- Secondly, dried sources of the BIPM solution were counted directly on the defined-angle detector, and the source self absorption was estimated [12] at (1.1 ± 0.2)% by noting the change in count rate when an electroplated source was dissolved on its mount (with a solution of the same acidity and solids content as the BIPM solution), dried and recounted.

4. Correction formulae for dead times

It was not considered worthwhile to record each participant's formula for the various methods, since the uncertainty in the correction involved is small relative to other parameters of uncertainty. Dead-time values and estimates of uncertainty due to dead time can be found in Tables 2 to 5 and in Table 7.

5. Results

The final results for N_o and N_{KX}, as well as their uncertainties (components of categories A and B, and combined in quadrature), are listed in Tables 6a and 6b. The components of category A are those which are evaluated by statistical methods, those of category B are evaluated by other means. A graphical representation is given in Fig. 3 and a histogram of the distribution in Fig. 4. In these figures, the N_{KX} values have been divided by 0.283, an estimate of $P_K\omega_K$ mentioned below. The various contributions to the estimated uncertainty components of category B are listed in Table 7 in the form of "standard deviations". All components of both categories are added in quadrature to give the combined uncertainty.

It is of interest to derive an experimental value of the quantity $P_K\omega_K$. Table 8 gives the weighted and unweighted means of N_o and N_{KX} for all measurements (except result number 8), as well as the means for N_o derived from the three results (numbered 4, 5 and 10) which were not dependent on theoretical estimates of P_K and ω_K. Experimental estimates of $P_K\omega_K$ are given by the ratio N_{KX}/N_o, and the value of 0.283 quoted above is the mean of the four estimates in the table.

6. Conclusion

Considering the many different methods of measurement chosen by the eleven participants, the spread in the results is rather less than was first anticipated. It was also expected, bearing in mind the relative difficulties involved, that the spread in the N_{KX} results would be less than the spread in the N_o results, but the opposite turned out to be the case. The spread in N_{KX} amounted to 7% whereas the spread in N_o amounted to 5% (omitting result number 8 which was 9% different from the mean). It is clear that most of the participants measuring N_{KX} underestimated their uncertainty components, as illustrated by the high value of $\chi^2/\nu = 7.6$, and as can also be deduced from Fig. 3. The most probable cause is an underestimate of the uncertainty involved in the relatively large self-absorption corrections.

Table 1 - List of the participants

		Names of the persons who carried out the measurements
AECL	Atomic Energy of Canada Limited Chalk River, Canada	J.S. Merritt, L.V. Smith, A.R. Rutledge
AIEA	International Atomic Energy Agency Vienna, Austria	H. Houtermans, N. Haselberger
BCMN	Bureau Central de Mesures Nucléaires Euratom, Geel, Belgium	R. Vaninbroukx, D. Reher, G. Grosse, A. Kacperek
IBJ	Instytut Badán Jadrowych Świerk, Poland	P. Zelazny, T. Radoszewski, T. Terlikowska, A. Chyliński
IMM	Institut de Métrologie D.I. Mendéléev Leningrad, USSR	F.M. Karavaev et al.
LMRI	Laboratoire de Métrologie des Rayonnements Ionisants, Saclay, France	R. Vatin
NAC	National Accelerator Centre Pretoria, South Africa	P. Oberholzer, J. Steyn
NBS	National Bureau of Standards Washington, D.C., USA	J.M.R. Hutchinson, B.M. Coursey
NPL	National Physical Laboratory Teddington, United Kingdom	D.H. Makepeace, D. Smith, M.J. Woods
NRC	National Research Council of Canada Ottawa, Canada	K. Munzenmayer, G.C. Bowes, A.P. Baerg
PTB	Physikalisch-Technische Bundesanstalt Braunschweig, Federal Republic of Germany	W. Pessara

Table 2 – Calibrated X-ray detectors to measure N_o

	1. Detector 2. Size 3. Resolution 4. Pulses counted by	1. Source backing 2. Wetting or seeding agent	1. ^{55}Fe dilution factor 2. Diluent 3. Final carrier content per g of solution	1. Number of sources 2. Typical mass 3. Count rate 4. Dead time	Variation with dilution	Special corrections applied	Measured nuclides	P_K	ω_K	$P_K\omega_K$
AECL (1)	1. Source sandwiched between 2 NaI(Tl) detectors at 5 mm from each 2. NaI is 5 cm diameter, 1 mm depth 3. 50% at 6 keV 4. SCA and scaler (2) SCA = 2.7 to 10.1 keV	1. Single VYNS 2. Catanac	1. 9.608 2. – 3. 2 µg	1. 7 (+ 1 undiluted) 2. 17 mg 3. 1 300 s^{-1} 4. 15 µs	Undiluted solution gave N_o about 0.27% lower than diluted solution	True summing corrections ^{51}Cr 0.5% ^{54}Mn 2.5% ^{57}Co 33.0%	^{51}Cr ^{54}Mn ^{55}Fe ^{57}Co	Assumed $P_K\omega_K$ varied linearly with atomic number		
BCMN (2)	1. Si(Li) detector 2. 2 cm^2 area, 3 mm depth 3. 600 eV 4. Counted with ADC + MCA	1. Pt coated glass disc 2. Ludox	1. 1, 2, 4, 8 2. 0.1 M HNO_3 3. 20, 7, 6, 2.5 µg	1. 12 2. 15 mg 3. 450 to 65 s^{-1} 4. Measured in live time of MCA	No systematic differences found between results at the four dilutions		^{51}Cr ^{54}Mn ^{55}Fe ^{57}Co ^{65}Zn	– – 0.886 – –	– – 0.314 – –	0.222 0.252 0.278 0.305 0.380
PTB (3)	1. Intrinsic Ge detector with cooled FET 2. 16 mm diameter, 5 mm depth 0.125 mm Be window 3. 270 eV at 6 keV 4. Counted with ADC + MCA	1. VYNS 2. Ludox for drop sources	1. None 2. None 3. 20 µg	Drop 1. 3; 2. 12 mg 3. 40 s^{-1}; 4. 0.7% Electroplated 1. 4; 2. 20 mg 3. 100 to 400 s^{-1} 4. 2 to 5%		Dead-time + Pile-up corrections by admixing artificial pulses	^{51}Cr ^{54}Mn ^{55}Fe ^{58}Co	0.892 0.889 0.885 0.886	(ω_K not used)	

SCA = single-channel analyser, MC = multichannel analyser, ADC = analog-to-digital converter, FET = field-effect transistor

All three laboratories incorporated source self absorption in their calibration curves and used references sources prepared in a similar manner with similar carrier concentrations as the ^{55}Fe.

AECL also ensured that the referenc sources gave a similar count rate as the ^{55}Fe, so any errors in dead time should cancel.

Table 3 – $4\pi\beta$-γ or $4\pi\beta$ methods to measure N_o

a) $4\pi\beta$(PC)-γ or $4\pi\beta$(PPC)-γ

	PC details (Ar–CH_4 filled) 1. Pressure (kPa) 2. Height 2πPC 3. Length wire 4. Diameter wire	Source backing 1. Nature 2. No. of films 3. " metal layers 4. Total mass ($\mu g\ cm^{-2}$)	Wetting or seeding agent (per g of water)	1. ^{55}Fe dilution factor 2. Diluent 3. Additional carrier 4. Final carrier (per g of solution)	Tracer nuclides	1. No. of sources 2. Typical mass 3. No. of data points for decay-scheme correction	Efficiencies 1. Range of N_c/N_γ 2. How altered 3. γ channel	Count rates 1. Beta and τ_β 2. Gamma and τ_γ 3. Coinc. and τ_R (s^{-1}), (μs)	P_K ω_K
NPL (4)	1. 100 2. 14 mm 3. 75 mm 4. 76 μm	1. VYNS 2. 1 3. 2 (Au) 4. ≈ 50 $\mu g/cm^2$ each	Catanac 50 μg Dried, rewetted with H_2O, dried in NH_3 atm.	1. None 2. None 3. None 4. 20 μg	^{51}Cr ^{54}Mn	1. 10 2. 25 mg 3. 37 (^{51}Cr) 4. 60 (^{54}Mn)	1. 10 to 57% 2. Sublimate NH_4Cl and/or add VYNS foils 3. Photopeak	1. < 50 000, 1.5 2. 10 000, 2.5 3. 5 000, 0.7	Not used
NRC (5)	1. 1 000 2. 25 mm 3. 38 mm 4. 25 μm	1. VYNS 2. 1 3. 2 (Au–Pd) 4. 40 each	Catanac SN 1 to 3 μg	1. 7.7 2. 0.1 M HNO_3 3. None 4. 3 μg	^{51}Cr ^{54}Mn	1. 18 2. 14 mg 3. 14	1. 30 to 70% 2. Pulse-height discrimination 3. Photopeak	1. 20 000) common 2. 500) 9.8, extending 3. 200 anticoincid. (no τ_R)	Not used
LMRI (6)	1. 700 2. 27.5 mm 3. 170 mm 4. 20 μm	1. Mylar 2. 2(top & bottom) 3. 2 (Al) 4. ≈ 400 each	None	1. None 2. None 3. None 4. 20 μg	^{54}Mn	1. 12 2. 20 mg 3. No extra-polation	1. ≈ 23.5% 2. Not altered 3. Photopeak	1. < 40 000) common 2. < 4 500) 5, extending 3. < 1 100, 1	^{54}Mn 0.894 0.286 ^{55}Fe 0.881 0.314

Table 3 (cont'd)

b) $4\pi\beta(LS)-\gamma$ or $4\pi\beta(LS)$

	1. Scintillator 2. Volume 3. Phototubes (β)	1. Adsorption check 2. After-pulse check	1. ^{55}Fe dilution factor 2. Diluent 3. Additional carrier 4. Final carrier (per g of scintillator)	Tracer nuclides	1. No. of sources 2. Typical mass 3. No. of data points for decay scheme correction	Efficiencies 1. Range of N_c/N_γ 2. How altered 3. γ channel	Count rates 1. Beta and τ_β 2. Gamma and τ_γ 3. Coinc. and τ_R (s^{-1}), (μs)	P_K ω_K
IMRI (7)	1. Butyl PBD, toluene, alcohol 2. 3 ml 3. 2 in summation	1. No, assumed 0% 2. Assumed 0%	1. two dilutions, 6 each 2. - 3. $FeCl_3$ 4. 8 μg	^{54}Mn	1. 6 at each dilution 2. 2.6 g ($\approx$ 15 mg active) 3. 12	1. 3 to 50% 2. Pulse-height discrimination 3. Photopeak	1. 10 000, 10 2. 1 200, 10 3. 600, 1	^{54}Mn 0.894 0.286 ^{55}Fe 0.881 0.314
IBJ (8)	1. PPO + bis MSD toluene triton X-100 2. 11 ml 3. 2 in coincidence (EMI 9634QR)	1. Yes 0% 2. Assumed 0%	1. 6.4, 8.0, 10.1 2. 20 μg/g Fe in 1 M HNO_3 3. 6%: 25 μg/g Fe in 0.1 M HCl 4. $\approx$ 1.5 μg	^{54}Mn	1. 12 2. 20 to 50 mg 3. 5 per source	1. 6 to 21% 2. Voltage variation 3. Photopeak	1. 5 000, 8 2. 250, 8 3. 50, 0.3	$^{54}Mn/^{55}Fe$ = 1.012 ω_K not used
NAC (9)	1. Instagel (Packard) 2. 12 ml 3. 2 in coincidence (RCA 8850)	1. Yes 0% 2. Yes 0.14% subtracted	1. 9.5 2. 50 μg/g $FeCl_3$ in 1 M HCl 3. None 4. $\approx$ 0.5 μg	^{51}Cr ^{54}Mn	1. 18 2. 100 mg 3. Not relevant	1. $\approx$ 50% 2. Light absorbers 3. Photopeak upwards	1. 40 000, 1.12 2. 180, 3.5 3. 90, 0.5	^{51}Cr 0.890 0.253 ^{54}Mn 0.889 0.283 ^{55}Fe 0.887 0.313
BCMN (10)	1. Lumagel or PPO-POPOP toluene-alcohol 2. 15 ml 3. 2 in coincidence or summation (RCA 8850)	1. Yes 0.2% 2. Assumed 0%	1. 2, 4, 8 2. 0.1 M HNO_3 3. None 4. 1 μg	None	1. 12 2. 15 mg 3. Not relevant	1. ε_c = 39%, 53% ε_s = 86%, 93% 2. Different scintillators 3. Not relevant	1. 12 000, 0.5 2. Not used 3. "	Not used

Table 4 - Methods with PPC (4π or 2π) to measure N_{KX}

	PC details ($Ar-CH_4$ filled) 1. Pressure (kPa) 2. Height 2πPC (mm) 3. Length wire (mm) 4. Diam. wire(μm) 5. " source mount (mm)	Source backing 1. Nature 2. No. of films 3. " metal layers 4. Total mass (μg cm^{-2})	Wetting or seeding agent	1. ^{55}Fe dilution factor 2. Diluent 3. Final carrier cont. (per g of solution)	1. No. of sources 2. Typical mass (mg) 3. Count rate (s^{-1}) 4. Dead time (μs)	1. Source self absorption (%) 2. How estimated?	1. Foil absorption (%) 2. How estimated?	Extrapolation to zero energy 1. Lower threshold (eV) 2. Correction (%) 3. How estimated?
4π counters								
BCMN (11)	1. 500 2. 80 3. 150 4. 21 5. 34	1. VYNS 2. 2 3. 2 (Au) 4. 100 each	Ludox	1. 80 2. 0.1 M HNO_3 3. 1 μg	1. 6 2. 15 3. 500 4. 4	1. 2 2. Auger [13] tracing	1. 5% 2. Calculation given thickness and density	1. 800 2. 0.3 3. Assumed flat spectrum
LMRI (12)	1. 1 000 2. 25 3. 190 4. 12 5. 38	1. Mylar 2. 2 3. 2 (Al) 4. 400 each	None, Dried in NH_3	1. None 2. None 3. 20 μg	1. 9 2. 10 to 15 3. 8 000 to 12 000 4. 5	1. 0.1 2. Computation (?)	1. ≈ 5% 2. Calculated	1. 500 2. 0.1 to 0.4 3. Assumed flat spectrum
NPL (13)	1. 500 2. 150 3. 300 4. 50 5. 75	1. Cellulose nitrate 2. 2 3. 2 (Al) 4. 150 each	Catanac 50 μg/g water. Dried, rewetted with water dried in NH_3	1. 6 2. 0.1 M HNO_3 3. 3 μg	1. 8 2. 25 3. 4 500 4. 15	1. 0.3 2. 'tracing' with ^{59}Fe beta Compare ε_β of ^{59}Fe and N_{KX} of ^{55}Fe from sources with and without Catanac	1. 2% 2. Calculation + addition of foils	1. 800 2. 0.3 3. Assumed flat spectrum

Table 4 (cont'd)

PC details ($Ar-CH_4$ filled) 1. Pressure (kPa) 2. Height 2πPC (mm) 3. Length wire (mm) 4. Diam. wire(μm) 5. " source mount (mm)	Source backing 1. Nature 2. No. of films 3. " metal layers 4. Total mass (μg cm^{-2})	Wetting or seeding agent	1. ^{55}Fe dilution factor 2. Diluent 3. Final carrier cont. (per g of solution)	1. No. of sources 2. Typical mass (mg) 3. Count rate (s^{-1}) 4. Dead time (μs)	1. Source self absorption (%) 2. How estimated?	1. Foil absorption (%) 2. How estimated?	Extrapolation to zero energy 1. Lower threshold (eV) 2. Correction (%) 3. How estimated?
4π counters							
IMM (14) 1. 600 2. 50 3. 150 4. 20 5. 20	1. "X-ray" film 2. 2 3. 2 (Al) 4. 155 each	Insulin + Ludox dried in NH_3	1. None 2. None 3. 20 μg	1. 11 2. 30 3. 10 000 4. 1 or 2	1. 0.5 2. Compare internal Bremsstrahlung with vacuum-evaporated source	1. 2% 2. Calculation + addition of foils	1. 500 2. 0.2% 3. Assumed flat spectrum
2π counters							
IMM (16) 1. ⩽ 100 2. ≈ 60 3. 120 4. 100 5. 20	"	"	"	"	"	"	"
AIEA (15) 1. 130-300 2. 90 3. ≈ 80 4. 25 5. ≈15	1. Celluloid 2. 1 covering source 3. 1 (Al) 4. 150	Electro-plated	1. None 2. None 3. 20 μg	1. 13 2. 6 to 20 equivalent 3. 3 000 to 10 000 4. 4	1. 0 (electroplated) 2. -	1. ≈ 3 2. Calculation + addition of foils	1. 1 000 2. Assumed 0 (?) 3. -

Table 5 - Defined solid angle [NaI(Tl)] detectors to measure N_{KX}

	Detector 1. Size 2. Window 3. Solid angle (sr) 4. Source detector	Source backing 1. Nature 2. No. of films 3. Mass ($\mu g\ cm^{-2}$)	^{55}Fe 1. Dilution factor 2. Final carrier cont. (per g of solution)	Wetting or seeding agent	1. No. of sources 2. Typical mass (mg) 3. Count rates (s^{-1}) 4. Dead time (μs)	Source self absorption (%)	Other calculated absorption corrections (%)	Extrapolation to zero energy (%)
LMRI (17)	1. 2 mm thick 2. 0.2 mm Be 3. ($1.865\ 8 \cdot 10^{-3}$) 4π 4. Filled with He gas	1. Mylar 2. 2 (top + bottom) 3. 400 each	1. None 2. 20 μg	None	1. 10 2. 28 to 42 3. 45 to 75 4. 5	< 0.05	0.8 foil 9 Be 3.3 Al 0.25 He	0 Empty spectrum below escape peak
NBS (18)	1. 1.6 mm thick 2. 0.13 mm Be 3. - 4. -	1. Stainless steel 2. No films 3. Sources not covered	1. None 2. 20 μg	Ludox (drops)	1. 5 2. 17-25 3. 100 4. MCA with accurate dead-time correction ($\tau \approx 5$)	1.1 measured (see text)	0 foil (not covered 5.6 Be 3.2 Al	3.92 ± 0.6 Assumed flat spectrum
				None (electro-plated)	1. 16 2. 17-50 equivalent 3. 300 4. As above	0		

Table 6a - Final results and uncertainties for N_o

Laboratory	Method	N_o Bq mg^{-1} on 1979-02-01	Uncertainties (standard deviations) (%)			
			Category A	Degrees of freedom	Category B	Combined
1. AECL	Calibrated NaI(Tl)	4 075	0.03	6	0.7	0.7
2. BCMN	Calibrated Si(Li)	3 970	0.2	15	1.9	1.9
	(+ ^{54}Mn only)	3 980	0.2	15	0.5	0.5
3. PTB	Calibrated germanium (drop)	4 040	0.2	17	0.8	0.8
	(electroplated)	4 060	0.6	23	1.0	1.2
4. NPL	4πβ(PC)-γ, efficiency tracing (+ ^{51}Cr)	4 065	0.2	13	0.9	0.9
	(+ ^{54}Mn)	3 932	1.2	15	1.1	1.7
	(+ ^{54}Mn)	3 954	0.8	81	0.8	1.2
5. NRC	4πβ(PPC)-γ, efficiency tracing (+ ^{51}Cr)	3 881	0.7	17	1.6	1.7
	(+ ^{54}Mn)	3 892	0.4	17	1.6	1.6
6. IMRI	4πβ(PPC)-γ, calculated efficiencies	4 020	0.3	11	2.6	2.6
7. IMRI	4πβ(LS)-γ, efficiency tracing	4 082	0.6	8	2.1	2.2
8. IBJ	4πβ(LS)-γ, efficiency tracing	4 348	0.6	(?)	0.1	0.6
9. NAC	4πβ(LS)-γ, calculated efficiencies (+ ^{51}Cr)	3 950	0.2	8	0.7	0.7
	(+ ^{54}Mn)	3 977	0.1	8	0.7	0.7
10. BCMN	4πβ(LS), coincidence + summing	4 040	1.0	11	1.1	1.5

Table 6b – Final results and uncertainties for N_{KX}

Laboratory	Method	N_{KX} $s^{-1}\,mg^{-1}$ on 1979-02-01	Uncertainties (standard deviations) (%)			
			Category A	Degrees of freedom	Category B	Combined
11. BCMN	4πβ(PPC)	1 123	0.5	3	0.5	0.7
12. IMRI	4πβ(PPC)	1 106	0.3	9	0.6	0.7
13. NPL	4πβ(PPC) (set 1)	1 143	0.2	5	1.0	1.0
	(set 2)	1 162	0.2	5	1.6	1.6
14. IMM	4πβ(PPC)	1 130	0.1	10	0.2	0.2
15. AIEA	2π(PPC)	1 161	0.1	12	0.4	0.4
16. IMM	2π(PPC)	1 128	0.1	10	0.3	0.3
17. IMRI	Defined solid angle [NaI(Tl)]	1 085	0.4	9	1.2	1.3
18. NBS	Defined solid angle [NaI(Tl)] (drop)	1 127	0.2	4	0.8	0.8
	(electroplated)	1 128	0.2	12	0.8	0.8

Table 7 - Uncertainty components (category B) in final result N_o (in %)

Laboratory	Method	Uncertainties (estimated standard deviations)		
1. AECL	Calibrated NaI(Tl)	a) interpolated efficiency	0.67	
			4 nuclides	Calibrated by ^{54}Mn only
2. BCMN	Calibrated Si(Li)	a) $P_K\omega_K$	1.8	0.5
		b) Tracer activity	-	0.1
		c) Efficiency (ratio)	0.7	0.1
		d) Others*	0.1	0.1
			Drop source	Electrolytic source
3. PTB	Calibrated Ge	a) P_K for ^{55}Fe	0.4	0.4
		b) Tracer activity	0.2	-
		c) Interpolated efficiency	0.6	0.8
		d) Pile up	-	0.3
		e) EC transition probability for ^{58}Co	0.3	0.3
			NPL	NRC
4. NPL	4πβ(PC)-γ eff. tracing	a) Extrapolation	0.8 to 1.1	0.3
		b) Tracer activity	0.3	0.4
5. NRC	4πβ(PPC)-γ eff. tracing	c) Source mixing	-	1.5
		d) Others*	0.1	0.25
			4πβ(PPC)-γ	4πβ(LS)-γ
6. LMRI	4πβ(PPC)-γ calcul.eff.	a) P_K	0.2	0.2
		b) ω_K	2.5	0.3
7. LMRI	4πβ(LS)-γ eff. tracing	c) t_K(PPC)	0.1	-
		d) f_K(PPC)	0.05	-
		e) p(LS)	-	0.5
		f) Extrapolation (LS)	-	2.0
		g) Others*	0.16	0.2
8. IBJ	4πβ(LS)-γ eff. tracing	a) Dead times	0.12	
		b) Tracer activity	-	
9. NAC	4πβ(LS)-γ calcul. eff.	a) Tracing procedure	0.68	
		b) Others*	0.16	
10. BCMN	4πβ(LS) coincid. and summing	a) Extrapolation	1.1	
		b) Stability	0.2	
		c) Others*	0.1	

Table 7 - Uncertainty components (category B) in final results N_{KX} (in %)

Laboratory	Method	Uncertainties (estimated standard deviations)				
			BCMN	LMRI	NPL	IMM
11. BCMN	4π(PPC)	a) Extrapolation to zero energy	0.1	0.1	0.1	0.02
12. LMRI	"	b) Self absorption	0.3	0.1	0.2	0.08
13. NPL	"	c) Foil absorption	0.3	0.56	1.0 to 1.6	0.07
14. IMM	"	d) Others*	0.1	0.2	0.05	0.14
				AIEA		IMM
15. AIEA	2π(PPC)	a) Extrapolation to zero energy		?		0.02
16. IMM	"	b) Self absorption		0		0.08
		c) Foil absorption		0.1		0.07
		d) Solid angle $\leqslant 2\pi$		0.4		?
		e) Others* (+ non-sphericity correction for IMM)		?		0.20
				LMRI		NBS
17. LMRI	Defined solid angle	a) Extrapolation to zero energy		0		0.6
18. NBS	"	b) Self absorption		0.05		0.2 (drop source)
		c) Be absorption		1.1		0.5
		d) Al absorption		0.4		
		e) He absorption		0.17		-
		f) Solid angle		0.1		0.1
		g) Others*		0.15		
		h) Intercomparison with liquid scint. (NBS)		-		0.2 (electrolytic sources)

* "Others" refers to uncertainty in dead times, weighing procedures, backgrounds, etc.

Table 8 - Mean values of activity and K X-ray emission rate at reference date (1979-02-01, 0 h UT)

		Weighted	Unweighted
N_{KX}	(s^{-1} mg^{-1})	1 132 ± 5 (7.6)	1 129 ± 7
N_o (all)	(Bq mg^{-1})	3 999 ± 15 (1.9)	3 995 ± 17
N_{KX}/N_o (all)		0.283 0 ± 0.001 5	0.282 7 ± 0.002 2
N_o (4, 5, 10)		3 984 ± 32 (2.2)	3 961 ± 31
N_{KX}/N_o (4, 5, 10)		0.284 1 ± 0.002 5	0.285 1 ± 0.002 6

The value following the ± sign is the combined uncertainty in the form of a standard deviation. The number in parentheses gives χ^2/ν, where ν is the number of degrees of freedom.

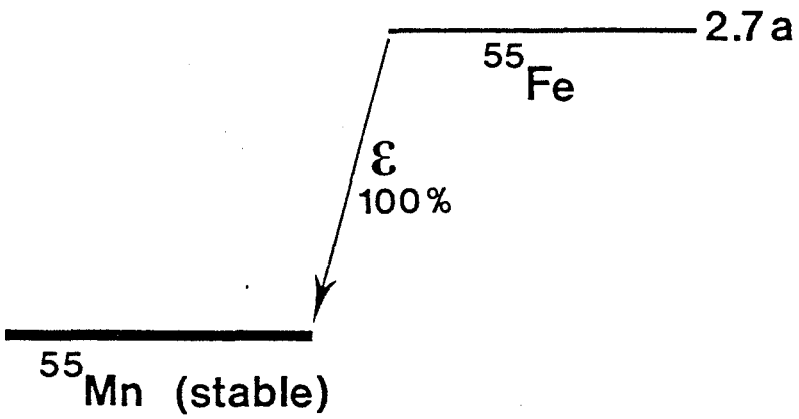

Fig. 1. - Decay scheme of ^{55}Fe

Fig. 2. - The curves illustrated on pages 25 to 29 represent functions for interpolation (versus atomic number) or extrapolation (versus 1 - ε_β, the inefficiency of the detector used). The number preceding the abbreviation for the laboratory refers to the method applied (see Tables 6a and 6b).

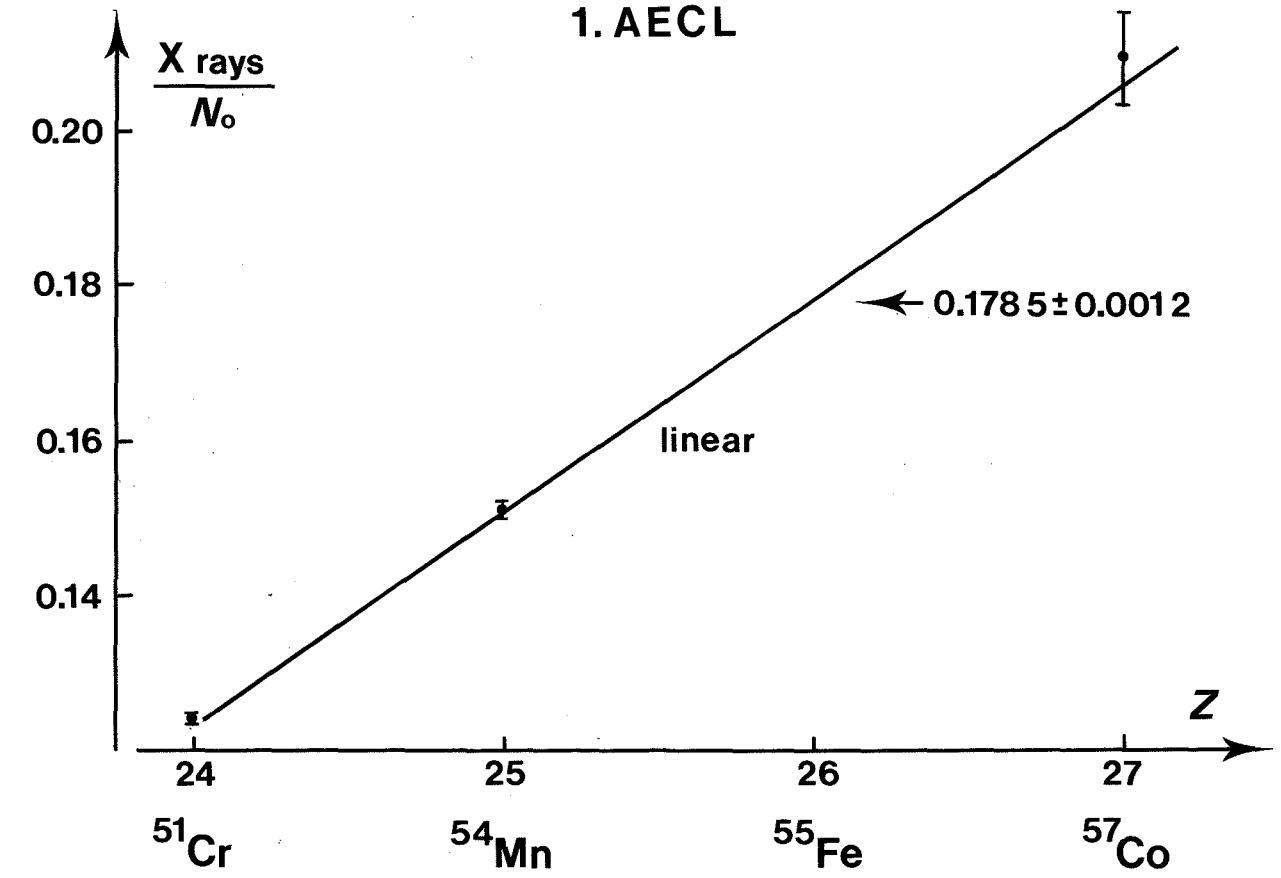
1. AECL
X rays / N₀
0.20
0.18
0.16
0.14
0.178 5 ± 0.001 2
linear
Z
24
25
26
27
51Cr
54Mn
55Fe
57Co

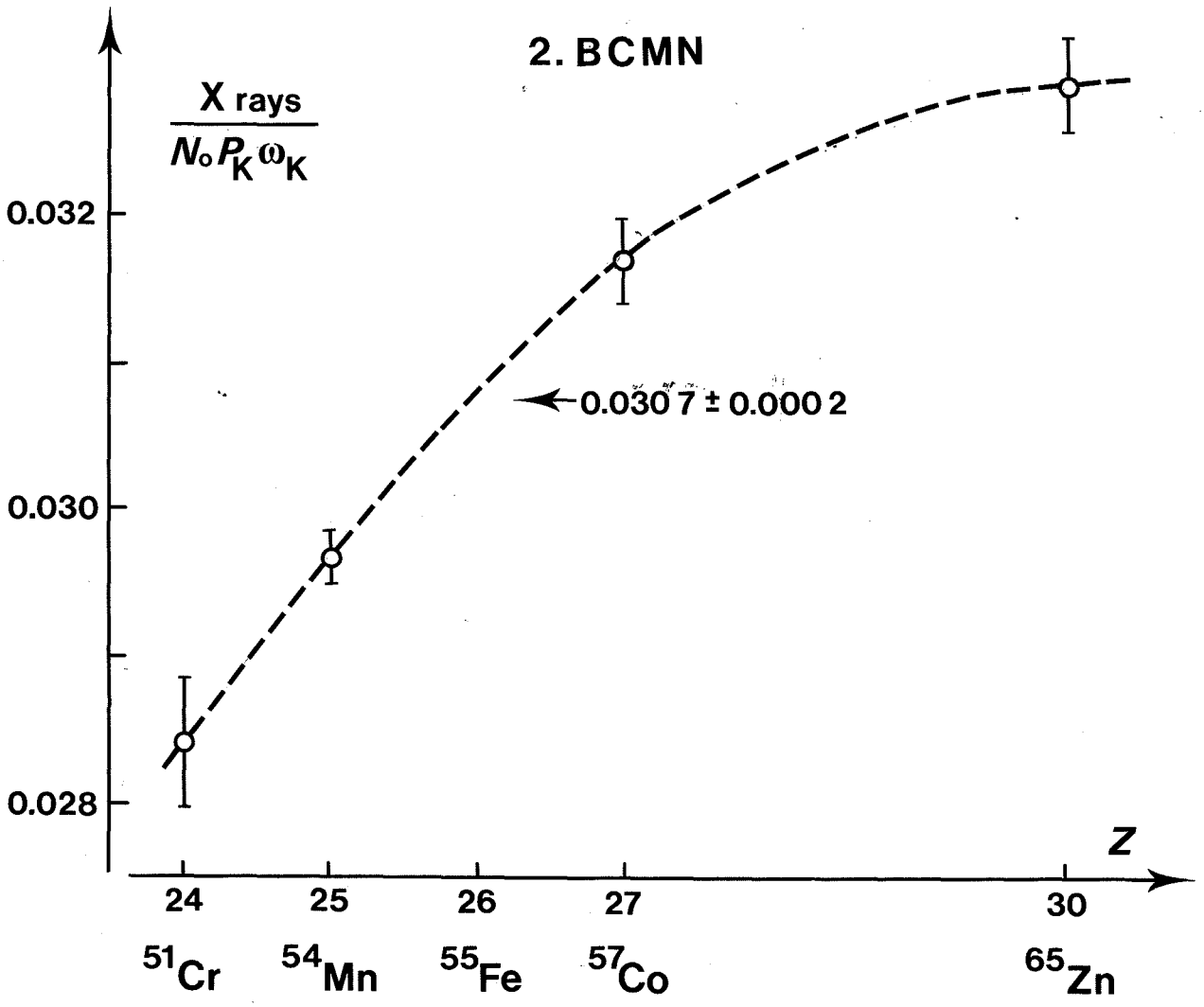
2. BCMN
X rays / N₀ P_K ω_K
0.032
0.030
0.028
0.030 7 ± 0.000 2
Z
24
25
26
27
30
51Cr
54Mn
55Fe
57Co
65Zn

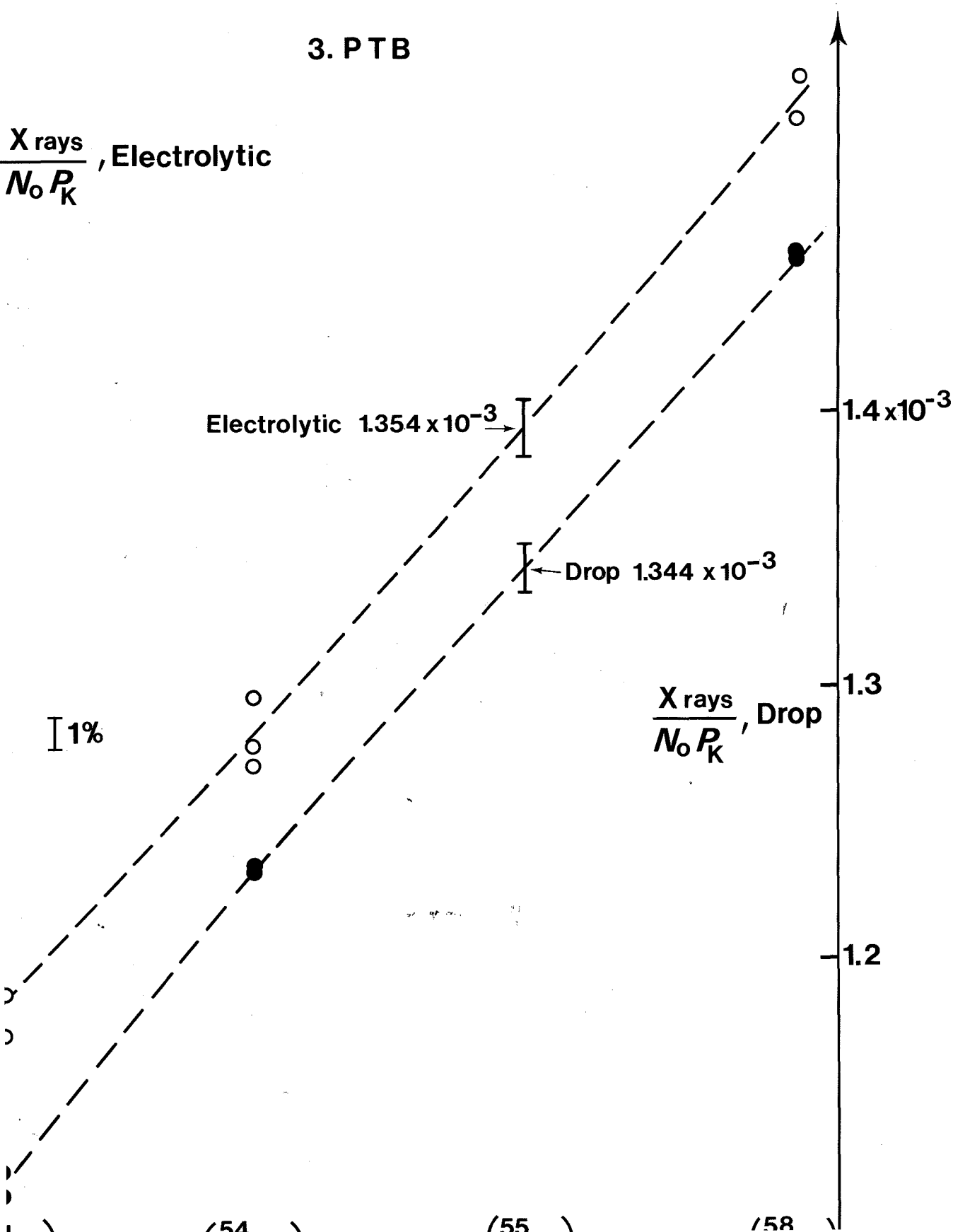
3. PTB
X rays / $N_o P_K$, Electrolytic
Electrolytic 1.354 x 10^{-3}
Drop 1.344 x 10^{-3}
1%
X rays / $N_o P_K$, Drop
1.4 x 10^{-3}
1.3
1.2

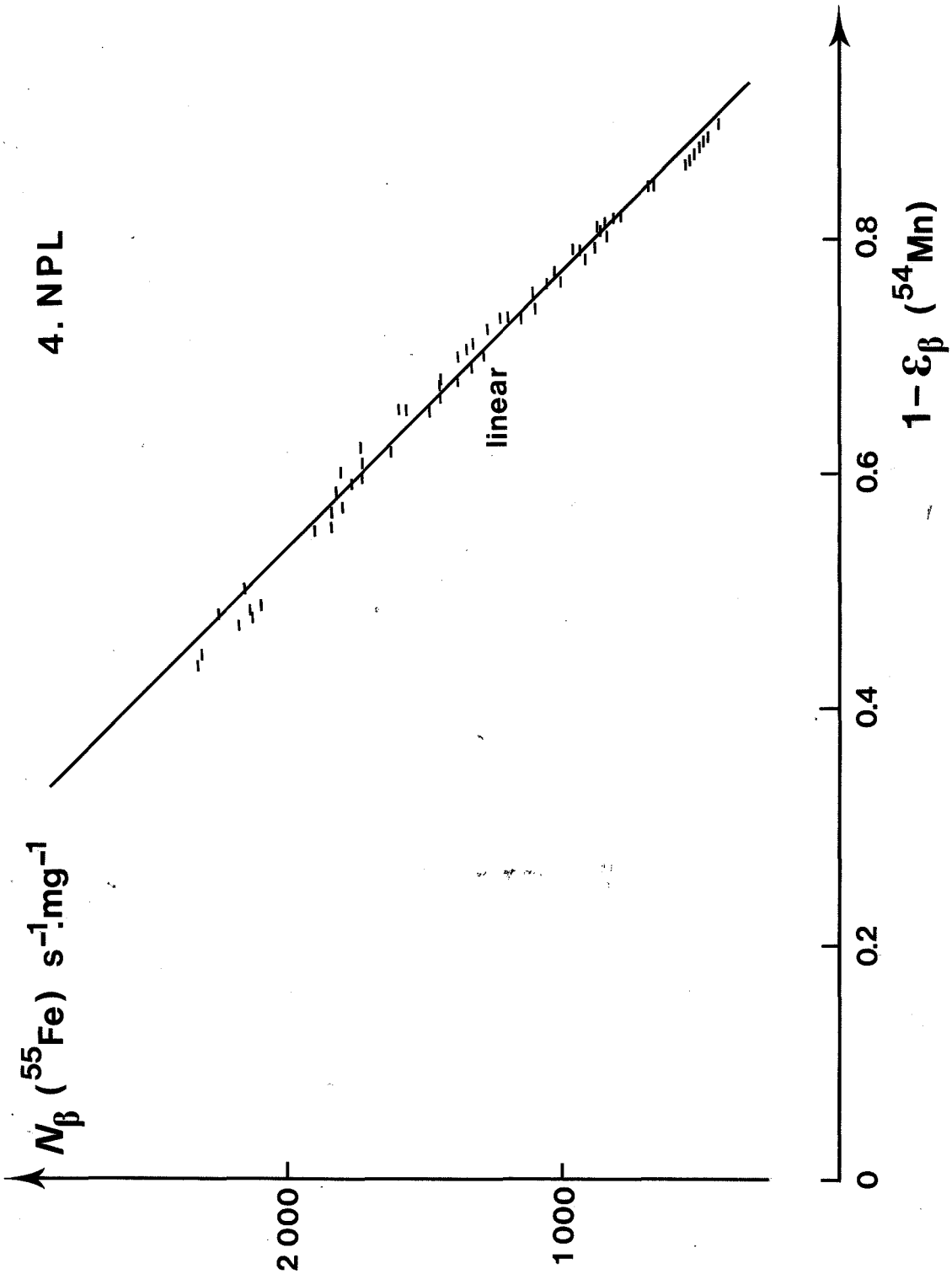
4. NPL
linear
N_β (^{55}Fe) s^{-1}.mg^{-1}
2 000
1 000
0
0.2
0.4
0.6
0.8
$1-\varepsilon_\beta$ (^{54}Mn)

5. NRC

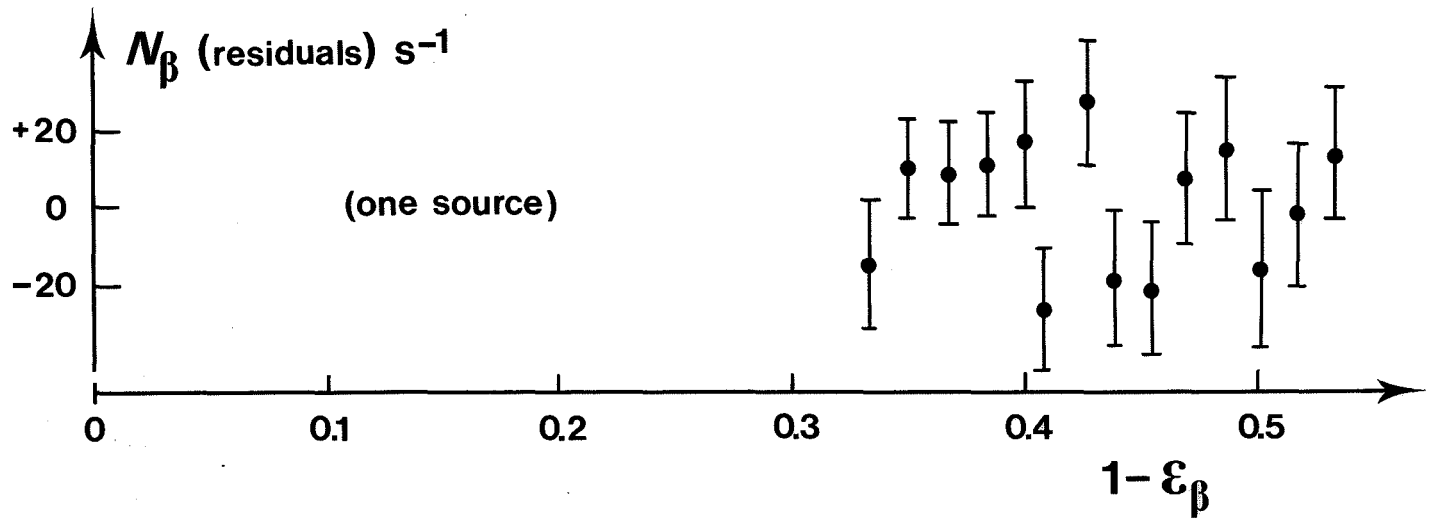
N_β (residuals) s^{-1}
+20
0
−20
(one source)
0
0.1
0.2
0.3
0.4
0.5
$1-\varepsilon_\beta$

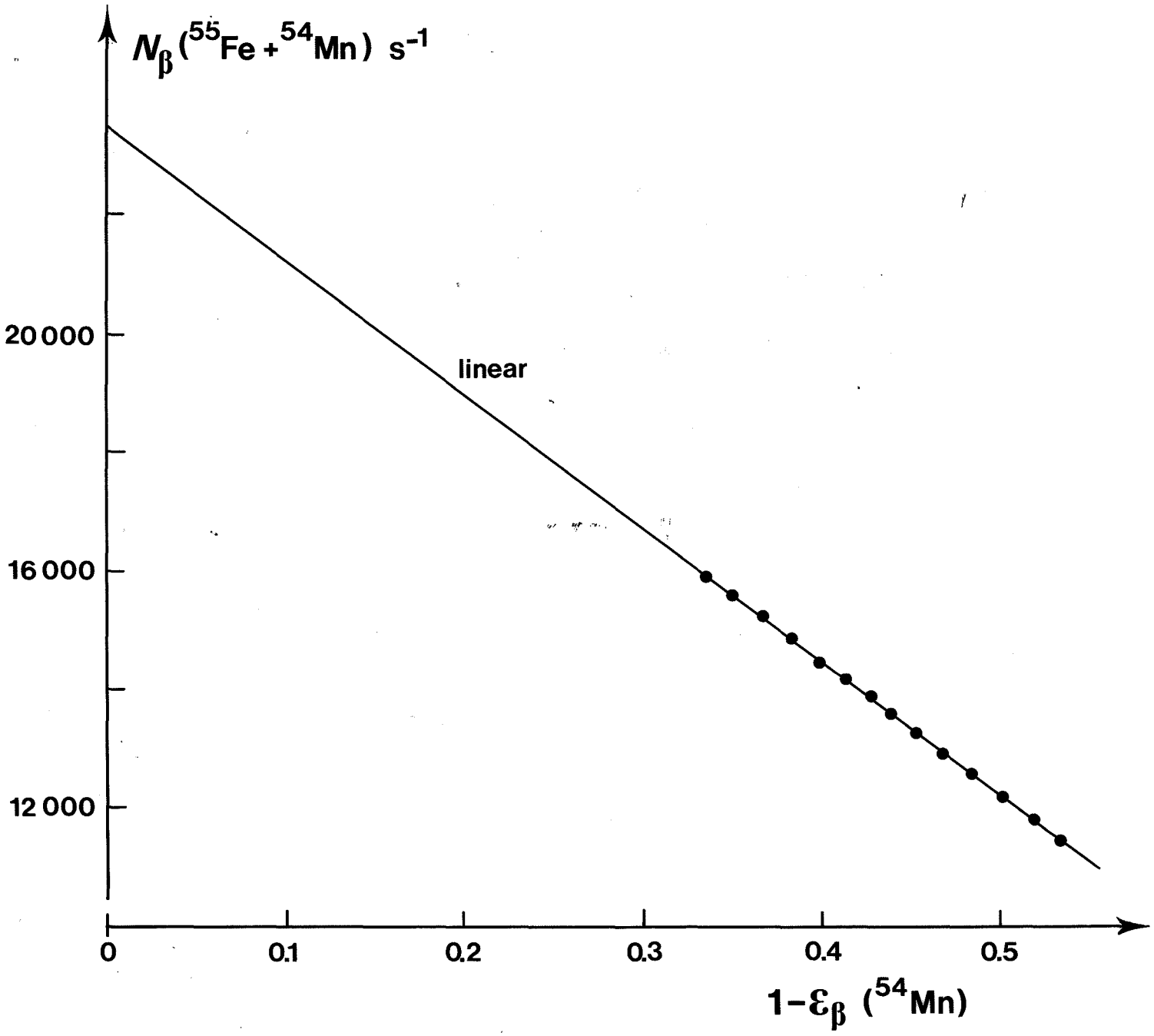
N_β (^{55}Fe + ^{54}Mn) s^{-1}
20 000
16 000
12 000
linear
0
0.1
0.2
0.3
0.4
0.5
$1-\varepsilon_\beta$ (^{54}Mn)

8. IBJ

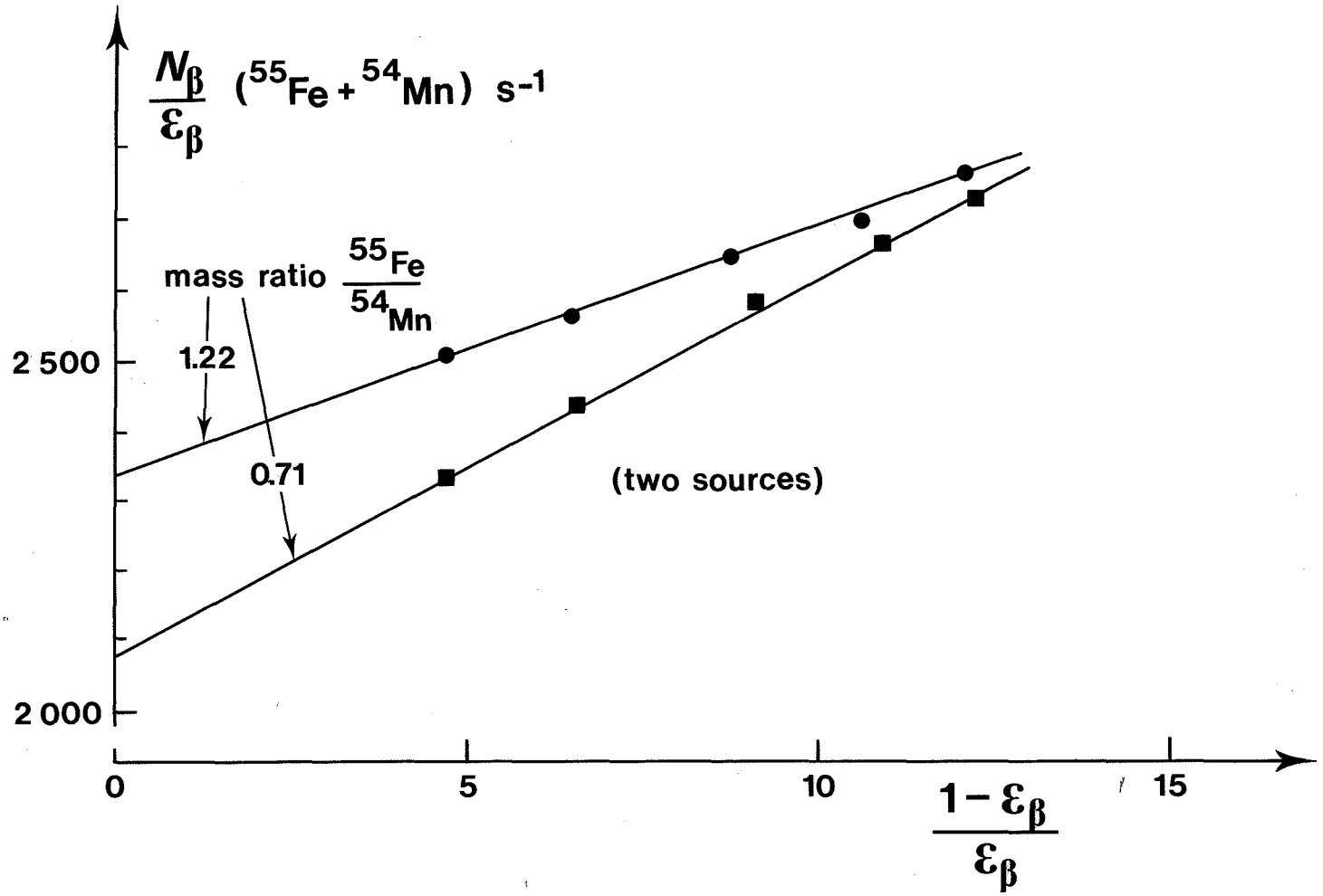
$\frac{N_\beta}{\varepsilon_\beta}$ (^{55}Fe + ^{54}Mn) s^{-1}
mass ratio $\frac{^{55}Fe}{^{54}Mn}$
1.22
0.71
(two sources)
2 500
2 000
0
5
10
15
$\frac{1-\varepsilon_\beta}{\varepsilon_\beta}$

10. BCMN

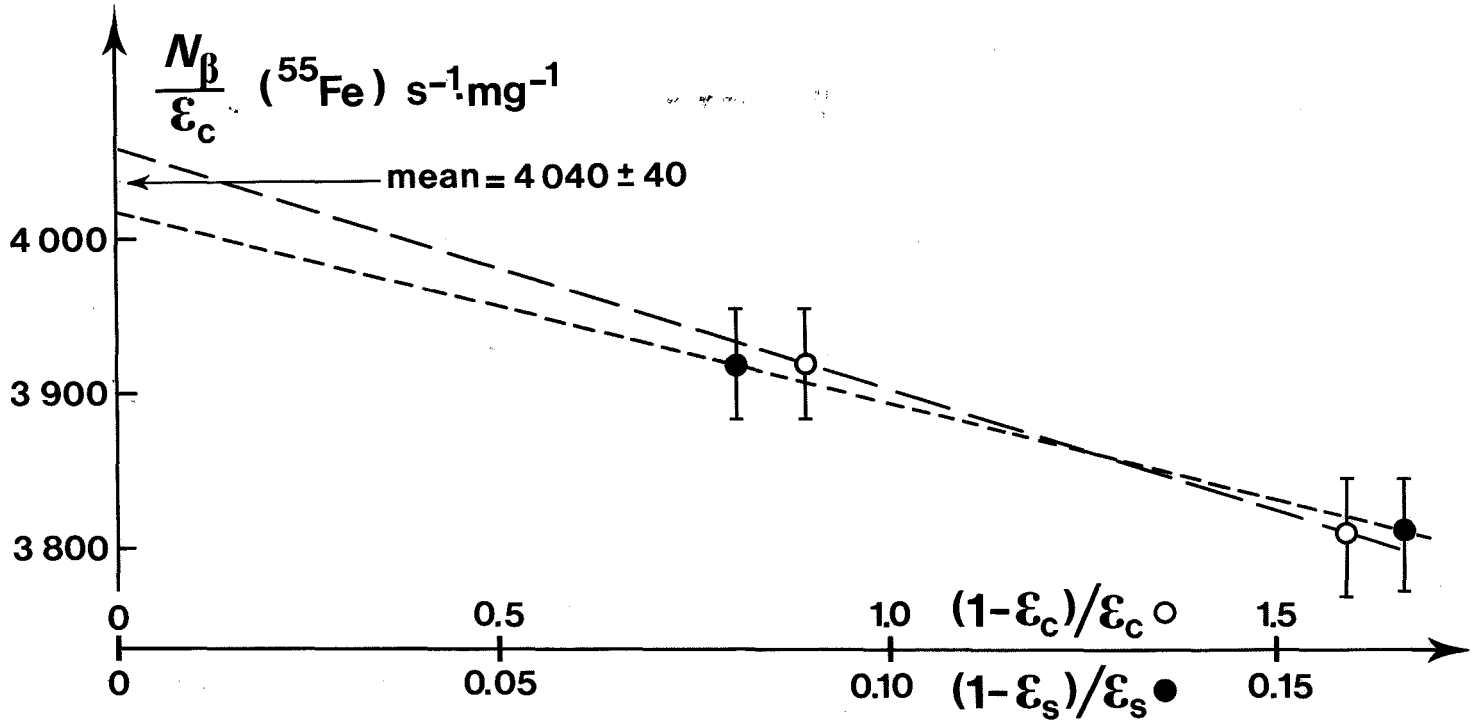
$\frac{N_\beta}{\varepsilon_c}$ (^{55}Fe) s^{-1}.mg^{-1}
mean = 4 040 ± 40
4 000
3 900
3 800
0
0.5
1.0
1.5
$(1-\varepsilon_c)/\varepsilon_c$ ○
0
0.05
0.10
0.15
$(1-\varepsilon_s)/\varepsilon_s$ ●

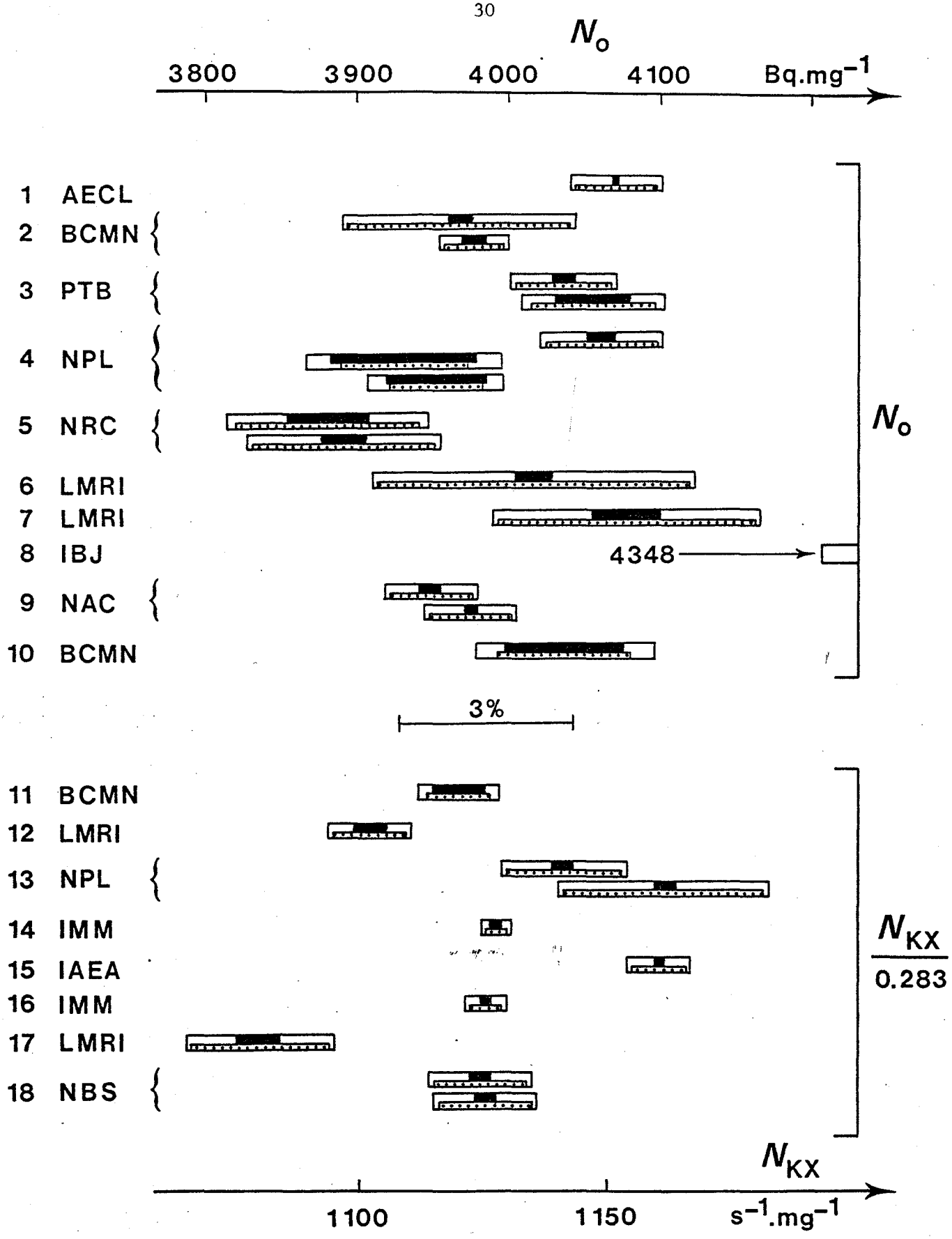

Fig. 3. - Graphical representation of the results. The reference date was 1979-02-01 0h UT. The black (or hatched or white) rectangles correspond to the random (or systematic or combined) uncertainties.

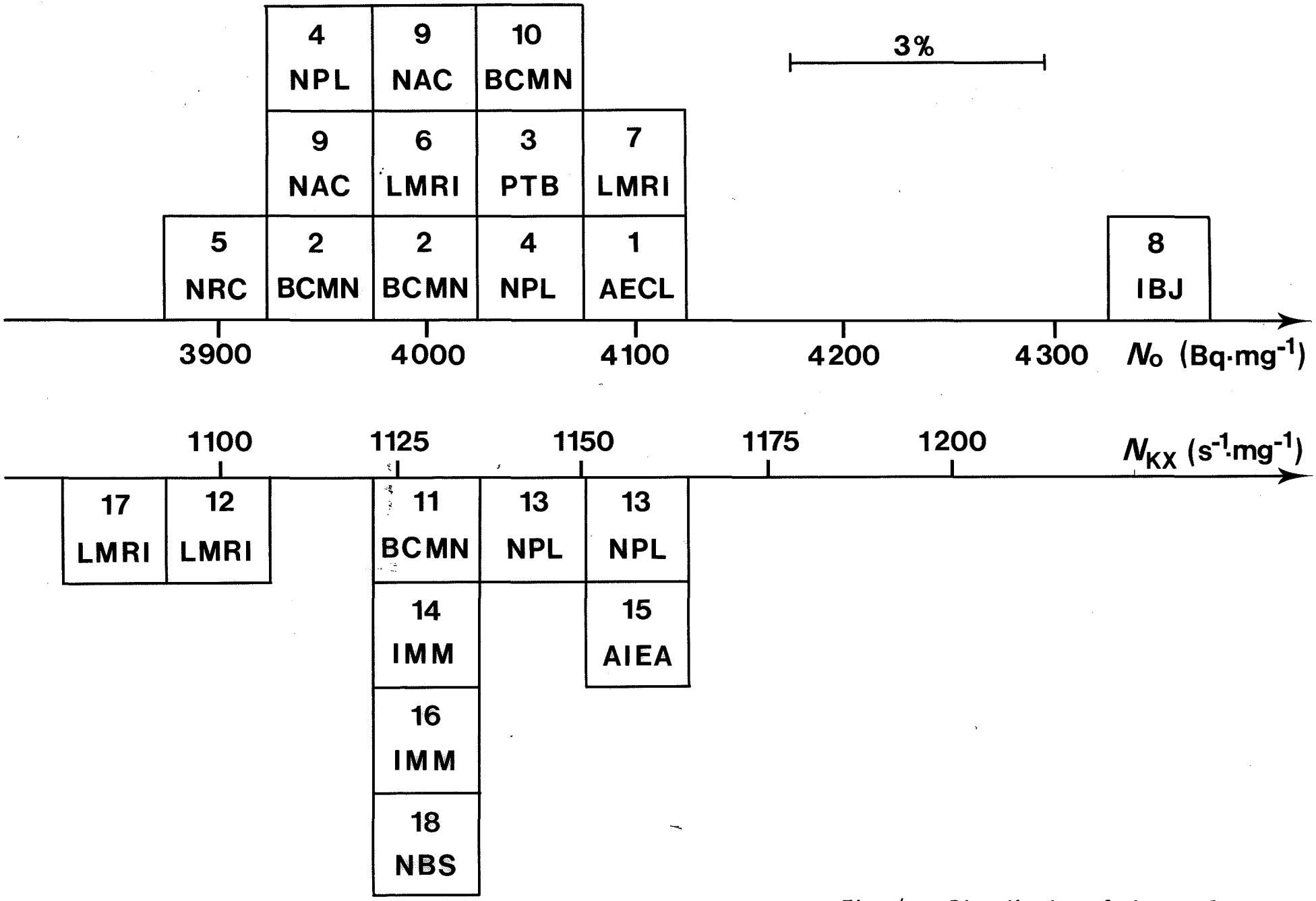

Fig. 4. - Distribution of the results

References

[1] J.W. Müller and A. Rytz, Report on the international comparison of dilution and source preparation methods by means of ^{60}Co, Part I: Results of the individual laboratories, (September 1967), in Recueil de Travaux du Bureau International des Poids et Mesures, Vol. I (1966-1967)

[2] A. Rytz, Report on the international comparison of activity measurements of a solution of ^{139}Ce (March 1976), Rapport BIPM-77/4

[3] A. Rytz, ^{134}Cs, Report of an international comparison of activity measurements (October 1978), Rapport BIPM-80/2

[4] A Handbook of radioactivity measurements procedures, NCRP Report No 58 (National Council on Radiation Protection and Measurements, Washington, 1978)

[5] K. Debertin and U. Schötzig, Coincidence summing corrections in Ge(Li)-spectrometry at low source to detector distances, Nucl. Instr. and Meth. 158, 471-477 (1979)

[6] M. Yoshida, H. Miyahara and T. Watanabe, A source preparation for $4\pi\beta$-counting with an aluminium compound, Int. J. Appl. Rad. and Isotopes 28, 633-640 (1977)

[7] A.P. Baerg, K. Munzenmayer and G.C. Bowes, Live-timed anti-coincidence counting with extending dead time circuitry, Metrologia 12, 77-80 (1976)

[8] J.A.B. Gibson and M. Marshall, The counting efficiency for ^{55}Fe and other EC nuclides in liquid scintillator solutions, Int. J. Appl. Rad. and Isotopes 23, 321-328 (1972)

[9] J. Steyn, P. Oberholzer and S.M. Botha, Accurate disintegration-rate measurement of ^{55}Fe by liquid scintillation counting, NAC/ST/79-01 (Pretoria, 1979)

[10] A.A. Konstantinov, Activity assays on electron-capture preparations, Priboni technika experimenta 1, 67 (1959)

[11] J.M.R. Hutchinson, W.B. Mann and P.A. Mullen, Development of the NBS low-energy-photon-emission-rate radioactivity standards, Proceedings ERDA Symposium on X- and Gamma-Ray Sources and Applications, Ann Arbor, Michigan, May 19-21, 1976

[12] S.B. Garfinkel and J.M.R. Hutchinson, Determination of source self-absorption in the standardisation of electron-capturing nuclides, Int. J. Appl. Rad. and Isotopes 13, 629-639 (1962)

[13] W. Bambynek and D. Reher, The self absorption of Auger electrons and X-rays in ^{54}Mn sources prepared by different methods, Int. J. Appl. Rad. and Isotopes 18, 19-24 (1967)